1   **A feasibility study on the bioconversion of CO_2 and H_2 to biomethane by gas sparging**

2   **through polymeric membranes**

3

4   I. Díaz[1*], C. Pérez[2], N. Alfaro[1], F. Fdz-Polanco[1]

5

6   [1]Department of Chemical Engineering and Environmental Technology, Escuela de

7   Ingenierías Industriales. Sede Dr. Mergelina.University of Valladolid. Dr. Mergelina s/n,

8   47011 Valladolid. Spain. Phone: +34983423166 Fax: +34983423013

9   [2]Department of Process Engineering. Ros Roca Indox Cryo Energy S.L. Spain.

10

NOTATION

$c_{Gmem_{H_2}}$	Concentration of H_2 in the stream supplied to the membrane (g/m³)
$c_{IN,G_{H_2}}$	Concentration of H_2 in the feed gas (g/m³)
$c_{L_{H_2}}$	Concentration of H_2 in the liquid phase (g/m³)
$c_{OUT,G_{H_2}}$	Concentration of H_2 in the effluent gas (g/m³)
f_X	Fraction of H_2 employed for microorganisms growth
H_{CH_4}	Dimensionless Henry's law constant for CH_4
H_{H_2}	Dimensionless Henry's law constant for H_2
$k_L a_{CO_2}$	Liquid film mass transfer coefficient for CO_2 (h⁻¹)
$k_L a_{H_2}$	Liquid film mass transfer coefficient for H_2 (h⁻¹)
$\dot{m}_{G \to L_{H_2}}$	Mass flow rate of H_2 transferred from gas to liquid phase (g/d)
$\dot{m}_{IN,G_{H_2}}$	Feed mass flow rate of H_2 gas (g/d)
$\dot{m}_{OUT,G_{CH_4}}$	Effluent mass flow rate of CH_4 gas (g/d)
$\left(\dot{m}_{OUT,G_{CH_4}}\right)_{H_2 eq}$	Effluent mass flow rate of CH_4 gas as equivalent H_2 according to equation 1 (g/d)
$\dot{m}_{OUT,G_{H_2}}$	Effluent mass flow rate of H_2 gas (g/d)
$\dot{m}_{OUT,L_{H_2}}$	Effluent mass flow rate of dissolved H_2 (g/d)
η_{H_2}	Efficiency of H_2 utilization (%)
OLR	Organic loading rate ($m^3_{H_2}/m^3_R$d)
$Q_{IN,G_{H_2}}$	Gas feed rate of H_2 (m³/d)
$Q_{RC,G}$	Gas recirculation rate (m³/d)
$Q_{OUT,G}$	Gas effluent rate (m³/d)
$Q_{OUT,G_{H_2O}}$	Gas effluent rate of water vapor (m³/d)
$r_{ut_{H_2}}$	H_2 utilization rate (g/h)
U	Specific substrate utilization rate (g_{COD}/g_{VSS}d)
$V_{m_{CO_2}}$	Molecular volume of CO_2 (mL/mol)
$V_{m_{H_2}}$	Molecular volume of H_2 (mL/mol)
V_R	Working volume of the bioreactor (L)
X	Concentration of microorganisms (g_{VSS}/L)
x_{CH_4}	Molar fraction of CH_4
Y_{CH_4}	Methane yield ($m^3_{CH_4}/m^3_{H_2}$)

11   *Author for correspondence: israel.diaz@iq.uva.es

12

13   **Abstract**

14   In this study, the potential of a pilot hollow-fiber membrane bioreactor for the conversion

15   of H_2 and CO_2 to CH_4 was evaluated. The system transformed 95% of H_2 and CO_2 fed at a

16   maximum loading rate of $40.2 m_{H_2}^3/m_R^3 d$ and produced 0.22 m^3 of CH_4 per m^3 of H_2 fed at

17   thermophilic conditions. H_2 mass transfer to the liquid phase was identified as the limiting

18   step for the conversion, and $k_L a$ values of $430 h^{-1}$ were reached in the bioreactor by sparging

19   gas through the membrane module. A simulation showed that the bioreactor could upgrade

20   biogas at a rate of $25 m^3/m_R^3 d$, increasing the CH_4 concentration from 60 to 95%v. This

21   proof-of-concept study verified that gas sparging through a membrane module can

22   efficiently transfer H_2 from gas to liquid phase and that the conversion of H_2 and CO_2 to

23   biomethane is feasible on a pilot scale at noteworthy load rates.

24

26

27   **1. Introduction**

28   The emissions of greenhouse gases are a major concern for environmental conservation as

29   they are directly linked to climate change; most of the recent global warming can be

30   attributed to the release of CO_2 and other heat-trapping gases from human activities (NRC,

31   2010). Decreasing CO_2 emissions can be achieved by reducing the amount of CO_2

32   produced and by managing the utilization of CO_2 or the storage and fossilization of CO_2

33 (Yang et al., 2008). Although technology that can increase the efficiency of combustion

34 processes and hence reduce the amount of fossil fuels burnt is evolving, only the

35 development of mitigation technologies can decrease the actual CO_2 concentration from its

36 current value (370 ppm) to the pre-industrial concentration (280 ppm). For this reason,

37 several technologies are subject of ongoing research to better capture, transform, utilize and

38 storage CO_2 (Mikkelsen et al., 2010), with a particular focus on biological alternatives, as

39 these can achieve carbon fixation with low or none use of chemical products, while also

40 avoiding extreme operational conditions, such as high pressure or temperature (Burkhardt

41 and Busch, 2013; Lam et al., 2012).

42

43 The technology to fix CO_2 by means of the chemoautotrophic conversion of CO_2 and H_2 to

44 biomethane (equation 1) by methanogenic *archaea* is still undeveloped because most of the

45 H_2 production worldwide comes from steam reforming of CH_4 (Ullman, 2000). However, it

46 is gaining attention in the actual context of renewable energies implementation. On the one

47 hand, H_2 production from wind and solar power through water electrolysis has been

48 proposed in order to circumvent the limitations of intermittency and site-specificity

49 associated with these sources (Levene et al., 2007). Furthermore, the low density of H_2

50 requires high storage volumes, and the technology for transportation and direct utilization is

51 still under development. As a consequence, its transformation to biomethane, which can be

52 injected into natural gas (NG) grids or employed as fuel for vehicles, is very attractive

53 (Deublein and Steinhauser, 2011). On the other hand, biogas production, with a typical

54 content of 60% CH_4 and 40% CO_2 from the anaerobic digestion (AD) of organic wastes

55 and by-products, is a well-established renewable energy technology in the EU

56 (EurObservER, 2013). Incentives and feed-in tariffs initially boosted electricity generation

57 from biogas, despite the low engines efficiency when using this feed, however recent cuts

58 and European policies to develop alternative fuels which reduce energetic dependence are

59 leading to the fast development of biogas upgrading plants that remove CO_2 and produce

60 biomethane (Petersson et al., 2007). By upgrading biogas with hydrogenotrophic *archaeas*

61 through equation 1, and an external source of H_2 from wind or solar power, a synergy could

62 be reached due to the fact that commercial upgrading plants are based on physical/chemical

63 processes (i.e. absorption, adsorption and membrane separation) that only separate CH_4

64 from CO_2, thus requiring further steps to avoid carbon emissions (Bauer et al., 2013).

65

66 $CO_2 + 4\ H_2 \rightarrow CH_4 + 2\ H_2O$ (eq. 1)

67

68 Literature shows two different approaches when considering the development of a

69 technology that takes advantage of hydrogenotrophic methanogenesis to remove CO_2.

70 Firstly, the addition of H_2 to anaerobic digesters of organic matter in order to remove CO_2

71 from biogas while increasing the production of biomethane (Luo and Angelidaki, 2013;

72 Luo et al., 2012; Wang et al., 2013) and, secondly, the supply of H_2 and a CO_2 (or biogas)

73 to an exclusively methanogenic bioreactor rich in hydrogenotrophic *archaeas* (Burkhardt

74 and Busch, 2013; Ju et al., 2008; Kim et al., 2013; Lee et al., 2012; Luo and Angelidaki,

75 2012; Peillex et al., 1990). Both lines of research found that the barrier to the successful

76 development of the technology on an industrial scale is the gas-liquid mass transfer of H_2,

77 due to its low solubility (dimensionless Henry's constant, $H_{H_2} = 50$ and $55\ g/L_G/g/L_{H_2O}$ at

78 35 and 55°C respectively (Ju et al., 2008)). Studies with gas diffusers on lab-scale CSTR

79 were shown to require high stirring speed; Peillex et al. (1990) attained an organic loading

80 rate (OLR) of 1488 $m_{H_2}^3/m_R^3 d$ with a methane yield of 0.19 $m_{CH_4}^3/m_{H_2}^3$ employing a pure

81 culture of *Methanobacterium thermoautotrophicum* at 65°C. More modest loads were

82 found when employing mixed methanogens cultures at thermophilic conditions (55°C)

83 (Luo and Angelidaki, 2012), increasing the content of CH_4 in biogas from 60 to 90% at a

84 rate of 14.4$m_{H_2}^3/m_R^3 d$. Another experiment with packed columns bioreactors reported a

85 load of 5.7$m_{H_2}^3/m_R^3 d$ with a mixed culture at mesophilic conditions obtaining a yield of

86 0.23$m_{CH_4}^3/m_{H_2}^3$ (Lee et al., 2012) (close to the stoichiometric maximum). Membrane

87 bioreactors (MBR) were also evaluated for the transfer of H_2 by gas diffusion through the

88 membrane material, reaching a final concentration of biomethane in upgraded biogas of

89 more than 95% (Strevett et al., 1995; Wang et al., 2013), as well as high methanogenic

90 activity even at low pH values or high concentrations of reaction intermediates (Ju et al.,

91 2008).

92

93 Literature on reactors with a working volume larger than 10L is scarce, and limited to

94 mesophilic temperature. Employing a 26.8L, Burkhardt and Busch (2013) found a yield of

95 0.26$m_{CH_4}^3/m_{H_2}^3$ in a trickled-bed bioreactor at a rate of 4.52$m_{H_2}^3/m_R^3 d$ and in Kim et al.

96 (2013) a load of 18$m_{H_2}^3/m_R^3 d$ was reached in a 100L CSTR at moderate stirring speed,

97 showing a slightly lower yield (0.23$m_{CH_4}^3/m_{H_2}^3$). Consequently, applied research should

98 focus on developing viable bioreactor configurations that achieve both a high load and a

99   high CH$_4$ yield on larger scales. This paper aims to study the feasibility of producing CH$_4$

100 from H$_2$ and CO$_2$ at thermophilic conditions on a pilot scale MBR.

101

102 **2. Materials and Methods**

103

104 2.1 Pilot plant description

105 One 40L cylindrical reactor (176mm x 1200mm) with a working volume of 31L was taken.

106 The reactor was insulated and the walls were heated with electric resistance. Feed gas was

107 obtained from gas cylinders, and the rate was regulated with rotameters. Feed line was

108 preheated in a thermostatic bath (55ºC), mixed with the recirculation, filtered by 0.45µm

109 (Millex, Millipore) and connected to the upper part of the membrane module as shown in

110 Figure 1. The hollow-fiber membrane module (Porous fibers, Spain) was placed in the

111 bioreactor to generate gas bubbles. The module consisted of 232 polymeric fibers (PVDF)

112 with a pore size of 0.4µm and fiber length of 550mm. The total membrane surface was

113 0.93m^2 and the module occupied 2.6L. The bioreactor was equipped with a gas pump to

114 recirculate biogas from the headspace through the membrane module, and one peristaltic

115 pump to mix the liquid at a constant rate of 700mL/min.

116

117 2.2 Operating conditions

118 The reactor was inoculated with 31L of anaerobic sludge from a thermophilic pilot plant

119 anaerobic digester at our laboratory treating activated sludge from Valladolid WWTP. We

120 set up the reactor by supplying H$_2$ and CO$_2$ (ratio according to equation 1) at an organic

6

121   loading rate of $5.03 m_{H_2}^3/m_R^3 d$ with a gas recirculation rate ($Q_{RC,G}$) of $0.10 m^3/d$ for 30d. All

122   the values of volumetric flow rates from the study are expressed at 55ºC and 1atm.

123

124   After the set-up period, the experiment started. The experiment was performed at

125   thermophilic conditions (55 ± 1ºC) and divided into 6 stages (I-VI), each corresponding to a

126   certain gas load rate, in order to determine the maximum OLR that could be applied with a

127   95% conversion efficiency for H_2 (η_{H_2}). Different $Q_{RC,G}$ were applied for some stages

128   (Table 1) in order to evaluate mass transfer conditions and reactor performance. Nutrients

129   required for microbial activity, and a phosphate buffer solution, were supplied when the

130   NH_4^+ concentration fell below 500 mg/L, specifically, during day 19, 52, 82 and 108.

131   200mL of macronutrients solution, 20mL of micronutrients solution diluted in 180mL of

132   distilled water and 200mL of buffer solution were added on the days mentioned. The

133   macronutrient solution was prepared like the stock solution A reported in Angelidaki and

134   Sanders (2004), while the micronutrients solution was a version that was modified (by

135   adding 500mg/L of resazurine) from the trace-metal solution also from Angelidaki and

136   Sanders (2004) and the phosphate buffer solution was prepared with $K_2HPO_4 \cdot 3H_2O$ and

137   KH_2PO_4 to a final pH of 7.2 with a concentration of 1mol/L PO_4^{3-}.

138

139   2.3 Monitoring and Experimental analysis

140   Headspace pressure was monitored with a Cerabar PMC131 probe (Endress Hauser) and

141   temperature was controlled with a PID and a PT100 probe. Effluent gas rate was measured

142   daily by liquid displacement, and gas composition (dry basis) was determined by gas

143 chromatography (GC-TCD) as described in Díaz et al. (2010). The liquid effluent was

144 collected and measured daily in a graduated cylinder.

145

146 Volatile fatty acids concentration was measured weekly by gas chromatography (GC-FID)

147 following the method reported in Alcántara et al. (2014).

148

149 Dissolved H_2 concentration ($c_{L_{H_2}}$) was measured periodically by gas –liquid partition with

150 a modified version of the method described in Yu et al. (2006). 8 mL of liquid were

151 sampled from the reactor and subsequently injected into a 10 mL gas-tight serological

152 bottle. The bottles contained 200μL of concentrated H_2SO_4 in order to prevent any

153 biological activity in the sample. They were closed with butyl septa, sealed with aluminum

154 caps and degassed with helium prior to the sample injection. H_2 in the headspace of the

155 bottles was measured 8h after sample injection by GC-TCD and liquid concentration was

156 estimated through mass balances. A higher variability between replicates is expected in this

157 modified version since analyses were only performed in duplicate in comparison to the

158 original method where triplicate aqueous samples were withdrawn. Due to the nature of the

159 GC detection limit for H_2 (1% in volume), the minimum $c_{L_{H_2}}$ that can be measured is

160 0.022mg/L.

161

162 pH, TSS (total suspended solids), VSS (volatile suspended solids) and NH_4^+ concentration

163 were measured weekly according to standard methods (APHA et al., 2005).

164

165 **3. Calculation**

166 Methane yield (Y_{CH_4}) was defined as the volume of CH4 generated per volume of H2 fed to

167 the bioreactor, and was calculated with equation 2. CH4 in the liquid effluent can be

168 neglected due to the low solubility of CH4 in water ($H_{CH_4} = 43$ at 55ºC) and the low liquid

169 effluent rate.

170 $$Y_{CH_4} = \left(Q_{OUT,G} - Q_{OUT,G_{H_2O}} \right) \cdot x_{CH_4} / Q_{IN,G_{H_2}} \qquad \text{(eq. 2)}$$

171 where $Q_{OUT,G}$ is the volumetric gas effluent rate, $Q_{OUT,G_{H_2O}}$ the volumetric flow rate of

172 water in the gas effluent (calculated with vapor pressure given by Antoine equation), x_{CH_4}

173 the molar fraction of CH4 (dry basis) in gas effluent and $Q_{IN,G_{H_2}}$ volumetric gas feed rate of

174 H2.

175 In a similar way, the efficiency of H2 utilization was defined by equation 3.

176 $$\eta_{H_2} = 100 \cdot \left(\dot{m}_{IN,G_{H_2}} - \dot{m}_{OUT,G_{H_2}} \right) / \dot{m}_{IN,G_{H_2}} \qquad \text{(eq. 3)}$$

177 where $\dot{m}_{IN,G_{H_2}}$ is the mass flow rate of H2 fed and $\dot{m}_{OUT,G_{H_2}}$ the mass flow rate of H2 in

178 the effluent gas. H2 in the liquid effluent can be neglected as well as it is several orders of

179 magnitude lower than the mass flow rates of H2 in gaseous streams.

180 A mass balance to the gas phase in the bioreactor (equation 4) was performed to calculate

181 the mass transfer coefficient for H2, $k_L a_{H_2}$

182 $$\dot{m}_{IN,G_{H_2}} = \dot{m}_{OUT,G_{H_2}} + \dot{m}_{G \to L_{H_2}} \qquad \text{(eq. 4)}$$

183 where $\dot{m}_{G \to L_{H_2}}$ is the mass flow rate of H2 transferred from the gas to the liquid phase in the

184 bioreactor. In steady-state conditions, $\dot{m}_{G \to L_{H_2}}$ is given by equation 5 assuming that all the

185 resistance to mass transfer is in the gas/liquid interphase.

186 $\dot{m}_{G \to L_{H_2}} = V_R \cdot k_L a_{H_2}(c_{Gmem_{H_2}}/H_{H_2} - c_{L_{H_2}})$ (eq. 5)

187 where $c_{L_{H_2}} \approx 0$ when the high turbulence provoked by gas sparging rate prevents a

188 concentration gradient in the liquid phase and dissolved H_2 is consumed completely by

189 methanogens. Then, combining eqs. 4 and 5, $k_L a_{H_2}$ can be obtained (equation 6)

190 $k_L a_{H_2} = \dfrac{\dot{m}_{IN,G_{H_2}} - \dot{m}_{OUT,G_{H_2}}}{V_R(c_{Gmem_{H_2}}/H_{H_2})}$ (eq. 6)

191 where V_R is the reactor working volume (31L). $c_{Gmem_{H_2}}$ is given by equation 7

192 $c_{Gmem_{H_2}} = \dfrac{c_{IN,G_{H_2}} \cdot Q_{IN,G} + c_{OUT,G_{H_2}} \cdot Q_{RC,G}}{Q_{IN,G} + Q_{RC,G}}$ (eq. 7)

193 $c_{IN,G_{H_2}}$ and $c_{OUT,G_{H_2}}$ are the H_2 concentrations in feed and effluent gas respectively, Q_{IN} the

194 volumetric gas feed rate and $Q_{RC,G}$ the volumetric gas recirculation rate.

195 Yu et al. (Yu et al., 2006) demonstrated that the mass transfer coefficient for a given

196 gaseous substrate can be estimated when the coefficient for a reference gas is known in the

197 same reactor and under the same operating conditions (equation 8); thus, the mass transfer

198 coefficient for CO_2 ($k_L a_{CO_2}$) was estimated.

199 $k_L a_{CO_2}/k_L a_{H_2} = \left(1/V_{m_{CO_2}}\right)^{0.4} / \left(1/V_{m_{H_2}}\right)^{0.4}$ (eq. 8)

200 where $V_{m_{H_2}}$ and $V_{m_{CO_2}}$ are the molecular volume of H_2 and CO_2 (14.3 and 34mL/mol

201 respectively) (Wilke and Chang, 1955).

202 From $\dot{m}_{G \to L_{H_2}}$, some parameters of the biological kinetics and stoichiometry were

203 calculated performing a mass balance to H_2 in the liquid phase of the bioreactor (equation

204 9)

205 $\dot{m}_{G \to L_{H_2}} = \dot{m}_{OUT,L_{H_2}} + r_{ut_{H_2}}$ (eq. 9)

206   where $r_{ut_{H_2}}$ is the H_2 utilization rate. From $r_{ut_{H_2}}$, U, the specific substrate utilization rate,

207   was obtained with equation 10 including the conversion factors: $8g_{COD}/g_{H_2}$ and 24h/d

208   $U = 0.33 \cdot r_{ut_{H_2}}/(X\,V_R)$ (eq. 10)

209   where X is the microorganisms concentration.

210   Finally, f_X, the fraction of H_2 employed for microorganisms growth (anabolism), was

211   estimated (equation 11) given the fact that the mass flow rate of H_2 consumed to produce

212   energy (catabolism) can be obtained from the methane production rate ($\dot{m}_{OUT,G_{CH_4}}$)

213   according to equation 1

214   $f_X = \dfrac{r_{ut,H_2} - \left(\dot{m}_{OUT,G_{CH_4}}/2\right)}{r_{ut,H_2}}$ (eq. 11)

215   where the term $\dot{m}_{OUT,G_{CH_4}}/2$ is defined as the mass flow rate of CH_4 as equivalent H_2

216   $\left(\dot{m}_{OUT,G_{CH_4}}\right)_{H_2\,eq}$ according to equation 1.

217

218   **4. Results and Discussion**

219

220   4.1. Performance of the conversion of H_2 and CO_2 to CH_4

221   The experiment started (stage Ia) with a $\dot{m}_{IN,G_{H_2}}$ of 22.9g/d and a $Q_{RC,G}$ of 0.10m³/d. The

222   mass balance performed to the gas phase (Figure 2a) showed that less than 90% of the H_2

223   fed was converted during these first days. Next, biogas recirculation rate was increased

224   stepwise according to Table 1 until 1.61m³/d, with the purpose of raising η_{H_2}. The

225   bioreactor presented an unstable behavior until day 20, η_{H_2} varied between 65% and 90%

226 (Figure 2b), and a we found a significant difference between $\dot{m}_{G \to L_{H_2}}$ and $\left(\dot{m}_{OUT,G_{CH_4}}\right)_{H_2 eq}$

227 until day 9, which indicates that a large part of the H_2 fed in these first days was transferred

228 to the liquid phase and consumed, but was not employed for CH_4 production, probably due

229 to biomass adaptation to the substrate. The bioreactor converted at least 95% of the H_2 fed

230 only after day 20. During stage Ie, the average η_{H_2} was 97% and the average Y_{CH_4} was

231 $0.20 m^3_{CH_4}/m^3_{H_2}$.

232

233 On day 27, $\dot{m}_{IN,G_{H_2}}$ was raised to 45.7g/d while $Q_{RC,G}$ was maintained at 1.61m³/d (stage

234 II). The increase in the mass flow rate provoked a slightly decrease in η_{H_2}, which remained

235 around 95% for this period, thus indicating that mass transfer conditions were still

236 acceptable even when the OLR was doubled. Besides, the average Y_{CH_4} was

237 $0.19 m^3_{CH_4}/m^3_{H_2}$, somewhat lower than at the end of the previous period. Given the fact that

238 the conversion efficiency did not substantially fall during stage II, we increased $\dot{m}_{IN,G_{H_2}}$ to

239 68.6g/d on day 40 (stage IIIa) and maintained $Q_{RC,G}$. In this case, η_{H_2} decreased to an

240 average 93% but the average Y_{CH_4} was not altered.

241

242 On day 58, $Q_{RC,G}$ was augmented to 2.41m³/d (stage IIIb). Under these conditions, the

243 performance of the bioreactor improved significantly, η_{H_2} reached 95% while Y_{CH_4}

244 increased to $0.23 m^3_{CH_4}/m^3_{H_2}$, much closer to the stoichiometric value. Furthermore, the

245 difference between $\dot{m}_{G \to L_{H_2}}$ and $\left(\dot{m}_{OUT,G_{CH_4}}\right)_{H_2 eq}$ was drastically lower than in previous

246   stages (Figure 2a) thus indicating that *archaeas* employed almost all H_2 transferred in order

247   to produce CH_4.

248

249   The maximum $\dot{m}_{IN,G_{H_2}}$ supplied to the bioreactor was 103g/d during stage IV, in

250   combination with a recirculation flow rate of 4.83m^3/d, the maximum capacity of gas

251   pump. Throughout this period, η_{H_2} never reached the targeted 95%, instead averaging 91%

252   while Y_{CH_4} was $0.21\text{m}^3_{CH_4}/\text{m}^3_{H_2}$. On day 98 (at the end of stage IV), the operation was

253   stopped and the bioreactor opened in order to observe the state of the membrane. There was

254   no biomass attachment to the membrane, in contrast to the biofilm found on the MBRs

255   employed for H_2 conversion to CH_4 in the literature (Ju et al., 2008; Wang et al., 2013),

256   which operated without gas bubbles, probably due to the turbulence provoked by the high

257   recirculation rates employed here to form bubbles while in Ju et al. (2008) and Wang et al.

258   (2013) gas diffusion through the membrane was the transference mechanism.

259

260   The operation was restarted a few hours later with $\dot{m}_{IN,G_{H_2}}$ of 57.2g/d (stage V). This

261   lower rate was chosen because during the technical stop some liquid was lost and replaced

262   with approximately 2 L of distilled water. η_{H_2} reached 96% after 2 days and Y_{CH_4} was

263    $0.23\text{m}^3_{CH_4}/\text{m}^3_{H_2}$, similar values to those found on stage IIIb with a comparable OLR. In

264   stage VIa, the rates of feed and recirculation were raised to 91.5g/d and 4.43m^3/d

265   respectively on day 111 and the maximum recirculation capacity was applied from day 124

266   (stage VIb). During stage VIb, η_{H_2} was 95% in average while the CH_4 yield was

267    $0.22\text{m}^3_{CH_4}/\text{m}^3_{H_2}$. In brief, the bioreactor successfully transformed at least 95% of the H_2 fed

268   at OLR between 10 and $40.2 m_{H_2}^3/m_R^3 d$ adjusting the gas recirculation rate and

269   $40.2 m_{H_2}^3/m_R^3 d$ is the maximum OLR that could be supplied to the system while converting

270   95% of the H_2 fed since the application of a higher loading rate (as in stage IV) failed to

271   achieve a such a conversion at the maximum recirculation rate provided by the gas pump.

272

273   This OLR is higher than that achieved on similar pilot-scale bioreactors, such as packed

274   column bioreactors ($4.5 m_{H_2}^3/m_R^3 d$) (Burkhardt and Busch, 2013) or CSTR ($18 m_{H_2}^3/m_R^3 d$)

275   (Kim et al., 2013); on the other hand, Y_{CH_4} was somewhat lower than in those experiments,

276   which found 0.26 and 0.23 $m_{H_2}^3/m_R^3 d$ respectively. Nevertheless, OLR during stage VIb

277   was more than double that applied in Kim et al. (2013), while the reactor yield decreased

278   only slightly. Hence, a membrane can be employed to transfer H_2 at a high rate, allowing

279   the biological conversion to take place satisfactorily. Further research should focus on the

280   long-term stability of the bioconversion rates found during this study.

281

282   4.2. Mass transfer capacity in the MBR

283   The concentration of dissolved H_2 in the liquid phase was below the detection limit during

284   the whole experiment (Figure 3). As a consequence, the assumption that all the resistance to

285   mass transfer is in the gas/liquid interphase was correct. The correlation coefficient

286   between the experimental data and the predicted values (equation 12) was 0.990, thus

287   confirming that H_2 mass transfer to the liquid phase can be described accurately by

288   equation 6 for the range of volumetric flow rates tested.

289

290     $k_L a_{H_2} = 0.0645(Q_{IN,G} + Q_{RC,G}) + 1.1866$ (eq. 12)

291

292   The $k_L a_{H_2}$ values observed (Figure 4) ranged from 30h^{-1} for the lowest total gas flow

293   through the membrane ($Q_{IN,G} + Q_{RC,G}$) to 430 h^{-1} (for the highest) and the estimated

294     $k_L a_{CO_2}$ from 20 to 300 h^{-1}.

295

296   It should be pointed out that this maximum $k_L a_{H_2}$ value is higher than $k_L a$ values found in

297   bioreactors with traditional gas diffusers (at equivalent gas rates), and in the range of CSTR

298   with high agitation speeds (700rpm) (Kreutzer et al., 2005). This is a consequence of the

299   large sparging area of the membrane module employed (sparging area to reactor working

300   volume ratio is 30m^2/m$_R^3$), however, this ratio is lower than employed by Wang et al.

301   (2013) when membranes were used to transfer H$_2$ by diffusion only (62m^2/m$_R^3$).

302   Conversely, gas sparging implies power consumption on gas recirculation to achieve a high

303     $k_L a_{H_2}$ while this power input is prevented when H$_2$ is transferred only by diffusion through

304   the membrane.

305

306   Conversely, much higher $k_L a$ values, as high as 3600 h^{-1}, were found in Peillex et al.

307   (1990) using H$_2$ diffusion through porous glass and a Rushton impeller; however, the

308   stirring speeds employed (over 1000 rpm) would presumably result in an extremely energy-

309   consuming system on a larger scale.

310

311　　A comparison between the maximum potential transfer rates ($k_L a(c_{Gmem}/H)$) from the gas

312　　to the liquid phase showed that the ratio $k_L a_{H_2}(c_{Gmem_{H_2}}/H_{H_2})/k_L a_{CO_2}(c_{Gmem_{CO_2}}/H_{CO_2})$

313　　is around $0.01 g_{H_2}/h/g_{CO_2}/h$ under the experimental conditions. This is another indicator

314　　of H_2 transfer limitations in the bioreactor because 0.18 g of H_2 is required per g of CO_2 to

315　　perform the conversion according to stoichiometry (Equation 1).

316

317　　4.3. Biological activity

318　　The maximum specific utilization rate (U) observed during the study was around

319　　$7 g_{COD}/g_{VSS}d$ (Figure 5). This experimental value is higher than the typical design value

320　　suggested for methanogens growing on H_2 and CO_2 ($2.2 g_{COD}/g_{VSS}d$) (Rittman, 2001).

321　　Nevertheless, a review of kinetic parameters for different pure cultures of hydrogenotrophic

322　　*archaea* showed that U ranges from $2-90 g_{COD}/g_{VSS}d$ depending on the specific strain

323　　(Pavlostathis and Giraldo-Gomez, 1991). The higher the U, the larger the H_2 rate that can

324　　be converted to CH_4 in a specific bioreactor before the reaction's limiting factors overtake

325　　the H_2 mass transfer. Therefore, U values found during this experiment appear not to be the

326　　potential maximum, and are limited by H_2 mass transfer in the system, since $c_{L_{H_2}}$ was

327　　always below the detection limit, indicating a lack of limitations for the biological reaction.

328

329　　A high $c_{L_{H_2}}$ inhibits propionate and butyrate conversion to acetate or H_2 and CO_2 during

330　　anaerobic digestion occasioning lower yields or the whole process breakdown (Speece,

331　　2008). Therefore, the fact that H_2 could be transferred at a high rate without any

332　　accumulation in the liquid phase is an important advantage of the technique studied, since it

333 might be applied to the own anaerobic digester, thus avoiding additional units for biogas

334 upgrading. In fact, in situ biogas upgrading was found feasible by Wang et al. (2013) where

335 H_2 was transferred only through diffusion and H_2 and CO_2 were partly consumed in the

336 biofilm developed over the membrane surface. Conversely, gas sparging impedes biofilm

337 formation and methanogenesis takes place totally in the bulk phase; then, additional

338 research is required to evaluate if $c_{L_{H_2}}$ would remain as low as in this experiment if

339 anaerobic digestion and upgrading were combined.

340

341 From another point of view, the adaptation of an unspecific anaerobic sludge to H_2 and CO_2

342 led to the development of an acclimated population for the production of biomethane with

343 yields of 0.22 $m_{CH_4}^3/m_{H_2}^3$ at 40.2$m_{H_2}^3/m_R^3$d and 0.23$m_{CH_4}^3/m_{H_2}^3$ at 30.2$m_{H_2}^3/m_R^3$d. These

344 yields are larger than the yields achieved employing specific strains of *Methanobacterium*

345 *Thermoautotrophicum* (Jee et al., 1988; Peillex et al., 1990) (0.19 and 0.18$m_{CH_4}^3/m_{H_2}^3$) or

346 *Methanococcus thermolithotrophicus* (Peillex et al., 1988) (0.16$m_{CH_4}^3/m_{H_2}^3$) at high η_{H_2}

347 values. This fact implies that the acquisition costs of specific strains of hydrogenotrophic

348 methanogens could be avoided on an industrial scale by employing unspecific anaerobic

349 sludge as inoculum instead, since higher yields could be reached, and given the fact that the

350 current process is limited by H_2 mass transfer.

351

352 The fraction of H_2 employed for methanogen growth (f_X) calculated with equation 11 was

353 larger during the first stages of the experiment than in the latter (Figure 5). f_X dropped

354 progressively from values around 0.7 at the beginning of the experiment to below 0.1 after

355   day 60. This result is supported by the fact that VSS concentration increased from 2.5g/L,

356   at the beginning of the study, to 3.6 g/L the day 58, and remained around this value during

357   the rest of the experiment (Figure 3). This was also the reason underlying the fact that Y_{CH_4}

358   was always below $0.20 \text{m}^3_{CH_4}/\text{m}^3_{H_2}$ until day 58, in spite of high η_{H_2} values, because an

359   important fraction of H_2 was utilized for microbial growth. Then, f_X was higher when

360   $\dot{m}_{G \to L_{H_2}}$ was low (also pointed by the important difference between $\dot{m}_{G \to L_{H_2}}$ and

361   $\left(\dot{m}_{OUT,G_{CH_4}}\right)_{H_2 eq}$ in the first stages) whereas it was lower when $\dot{m}_{G \to L_{H_2}}$ rose, thus

362   indicating an uncoupling of microbial growth (anabolism) and H_2 conversion to CH_4

363   (catabolism). This finding is in agreement with Fardeau and Belaich, (1986) and with

364   Schönheit et al. (1980), where this phenomenon had already been reported. An extensive

365   discussion about not fixed stoichiometry in methanogenic environments from a biochemical

366   point of view can be found in Kleerebezem and Stams (2000). Additionally, since the

367   inoculum employed in this study was adapted to the treatment of activated sludge prior to

368   the beginning of the study, only a small fraction of the original microbial community was

369   employed for the transformation of H_2 and CO_2 during the experiment. This fact may

370   influence stoichiometry as well, especially on the first stages, and molecular biology tools

371   should be considered in further research in order to elucidate how the evolution of the

372   microbial community influences the methane yield obtained.

373

374   From a technological point of view, the repercussions that arise from uncoupled growth and

375   conversion are, at least initially, positive. A bioreactor can be inoculated and biomass

376   adapted from an anaerobic sludge (treating a different substrate) directly inside the

377   methanogenic bioreactor in a short period (as in this study). A low OLR can be used, and

378   an important fraction of H_2 and CO_2 will be employed for methanogens growth. Once the

379   desired biomass concentration is achieved, OLR can be raised, while most of the substrate

380   will be employed for CH_4 production.

381

382   VFA concentration was very low during the whole experiment. Acetic acid concentration

383   was under 100mg/L, propionic acid was below 50 mg/L, and only traces of butyric acid

384   were found. These concentrations are probably the result of microbial decay and

385   endogenous activity. Acetate might also be produced, to some extent, by homoacetogenic

386   bacteria, which use H_2 to reduce CO_2 to produce acetate. However, methanogenesis

387   outcompeted homoacetogenesis in the present study, in contrast to Ju et al. (2008), where a

388   VFA concentration over 4000mg/L was found in combination with acetoclastic and

389   hydrogenotrophic methanogenesis.

390

391   4.4 Application of the MBR for biogas upgrading

392   The biomethane concentration in upgraded biogas was simulated by assuming that the

393   MBR studied here were employed for the upgrading of biogas under the following

394   conditions:

395   (i) $k_L a_{H_2}$ values at similar volumetric flow rates through the membrane are the same

396   when feeds of biogas and H_2, and of pure CO_2 and H_2 are fed, since $k_L a$ is not

397   dependent on the concentration of each compound

398 (ii) $Q_{IN,G} + Q_{RC,G}$ must fall within the range of studied rates so that the $k_L a_{H_2}$ values can

399   be calculated with equation 12 ($Q_{IN,G} + Q_{RC,G} < 6.6 \text{m}^3/\text{d}$).

400 (iii) f_X is the same for biogas feed because the additional CH_4 supplied to the system will

401   not alter the microbial activity (the concentration of dissolved CH_4 is that

402   corresponding to the equilibrium in both cases)

403 (iv) the CO_2 rate supplied as biogas and the H_2 rate are the same than those in stage VI of

404   the experiment (the maximum OLR that could be applied while achieving a 95%

405   bioconversion efficiency of H_2)

406

407 The simulation was carried out using the mass balance equations for gas (equations. 4 and

408 5) and liquid phases (eqs. 9 and 11), where the unknown variables are $\dot{m}_{OUT,G_{CH_4}}$ and

409 $c_{OUT,G_{H_2}}$. f_X employed was 0.07, the average value found in the experiment after day 60

410 and $k_L a_{H_2}$ was calculated with equation 12.

411

412 The volumetric flow rates of biogas that could be upgraded with an equivalent CO_2 content

413 to that of stage VI were 20m^3 /m$_R^3$d (50/50 CH_4/CO_2), 25m^3 /m$_R^3$d (60/40) and

414 34m^3 /m$_R^3$d (70/30). The final CH_4 concentration as a function of recirculation to feed

415 ratio was represented in Figure 6. Ratios between 1.75 and 2.25 were required to reach a

416 95%v. concentration of CH_4 and this was the maximum concentration achievable to comply

417 with condition (ii). However, this upgraded biogas fulfills the requirements for grid

418 injection or for utilization as vehicle fuel in most European countries according to

419 Petersson et al. (2007).

420

5. Conclusions

The bioconversion of H_2 and CO_2 to CH_4 was feasible at a maximum loading rate of

$40.2 m^3_{H_2}/m^3_R d$ while achieving a 95% efficiency in H_2 utilization. Gas sparging through

the membrane resulted in a large capacity of H_2 mass transfer in the range of high-speeds-

stirring lab-scale bioreactors. Methanogens showed higher ratios of conversion when the

load rate was increased, which entails a technological advantage when developing an

efficient methanogenic population during the start-up, at low load rates, while increasing

energy conservation at high load rates. The system could upgrade biogas efficiently

reaching a final concentration of biomethane of 95%v.

7. References

1. Alcántara, C., Fernández, C., García-Encina, P., Muñoz, R., 2014. Mixotrophic

metabolism of Chlorella sorokiniana and algal-bacterial consortia under extended dark-light

periods and nutrient starvation. Appl. Microbiol. Biotechnol. 99, 2393-2404.

2. Angelidaki, I., Sanders, W., 2004. Assessment of the anaerobic biodegradability of

macropollutants. Rev. Environ. Sci. Bio/Technology 3, 117–129.

441   3. APHA, AWWA, WPCF, 2005. Standard Methods for the Examination of Water and

442   Wastewater, 21st ed., Washington, DC.

443   4. Bauer, F., Hulteberg, C., Persson, T., Tamm, D., 2013. Biogas upgrading – Review of

444   commercial technologies (Biogasuppgradering – Granskning av kommersiella tekniker).

445   Report from the Swedish Gas Technology Center, Malmö.

446   5. Burkhardt, M., Busch, G., 2013. Methanation of hydrogen and carbon dioxide. Appl.

447   Energy 111, 74–79.

448   6. Deublein, D., Steinhauser, A., 2011. Biogas from Waste and Renewable Resources: An

449   Introduction. Wiley.

450   7. Díaz, I., Lopes, a C., Pérez, S.I., Fdz-Polanco, M., 2010. Performance evaluation of

451   oxygen, air and nitrate for the microaerobic removal of hydrogen sulphide in biogas from

452   sludge digestion. Bioresour. Technol. 101, 7724–30.

453   8. EurObservER, L'Observatoire des energies renouvelables, 2013. The state of renewable

454   energies in europe. ISSN 2101-9622

455   9. Fardeau, M., Belaich, J., 1986. Energetics of the growth of Methanococcus

456   thermolithotrophicus. Arch. Microbiol. 144, 381–385.

457   10. Jee, H.S., Nishio, N., Nagai, S., 1988. Continuous CH4 Production from H2 and CO2

458   by Methanobacterium thermoautotrophicum in a fixed-bed reactor. J. Ferment. Technol. 66,

459   235–238.

460   11. Ju, D., Shin, J., Lee, H., Kong, S., 2008. Effects of pH conditions on the biological

461   conversion of carbon dioxide to methane in a hollow-fiber membrane biofilm reactor (Hf –

462   MBfR). Desalination 234, 409–415.

463 12. Kim, S., Choi, K., Chung, J., 2013. Reduction in carbon dioxide and production of

464 methane by biological reaction in the electronics industry. Int. J. Hydrogen Energy 38,

465 3488–3496.

466 13. Kleerebezem, R., Stams, a J., 2000. Kinetics of syntrophic cultures: a theoretical

467 treatise on butyrate fermentation. Biotechnol. Bioeng. 67, 529–43.

468 14. Kreutzer, M.T., Kapteijn, F., Moulijn, J.A., Ebrahimi, S., Kleerebezem, R., Loosdrecht,

469 M.C.M. Van, 2005. Monoliths as Biocatalytic Reactors : Smart Gas - Liquid Contacting for

470 Process Intensification. Ind. Eng. Chem. Res. 9646–9652.

471 15. Lam, M.K., Lee, K.T., Mohamed, A.R., 2012. Current status and challenges on

472 microalgae-based carbon capture. Int. J. Greenh. Gas Control 10, 456–469.

473 16. Lee, J.C., Kim, J.H., Chang, W.S., Pak, D., 2012. Biological conversion of CO2 to CH4

474 using hydrogenotrophic methanogen in a fixed bed reactor. J. Chem. Technol. Biotechnol.

475 87, 844–847.

476 17. Levene, J.I., Mann, M.K., Margolis, R.M., Milbrandt, A., 2007. An analysis of

477 hydrogen production from renewable electricity sources. Sol. Energy 81, 773–780.

478 18. Luo, G., Angelidaki, I., 2012. Integrated biogas upgrading and hydrogen utilization in

479 an anaerobic reactor containing enriched hydrogenotrophic methanogenic culture.

480 Biotechnol. Bioeng. 109, 2729–2736.

481 19. Luo, G., Angelidaki, I., 2013. Co-digestion of manure and whey for in situ biogas

482 upgrading by the addition of H2: process performance and microbial insights. Appl.

483 Microbiol. Biotechnol. 97, 1373–81.

484   20. Luo, G., Johansson, S., Boe, K., Xie, L., Zhou, Q., Angelidaki, I., 2012. Simultaneous

485   hydrogen utilization and in situ biogas upgrading in an anaerobic reactor. Biotechnol.

486   Bioeng. 109, 1088–1094.

487   21. Mikkelsen, M., Jørgensen, M., Krebs, F.C., 2010. The teraton challenge. A review of

488   fixation and transformation of carbon dioxide. Energy Environ. Sci. 3, 43-81.

489   22. NRC, The National Research Council, 2010. Advancing the Science of Climate

490   Change. A report from The National Academies, Washington, DC.

491   23. Pavlostathis, S.G., Giraldo-Gomez, E., 1991. Kinetics of anaerobic treatment . Water

492   Sci. Technol. 24, 35–59.

493   24. Peillex, J., Fardeau, M., Boussand, R., Navarro, J., Belaich J.P., 1988. Growth of

494   Methanococcus thermolithotrophicus in batch and continuous culture on H2 and CO2:

495   influence of agitation. Appl. Microbiol. Biotechnol. 29, 560–564.

496   25. Peillex, J.-P., Fardeau, M.-L., Belaich, J.-P., 1990. Growth of Methanobacterium

497   thermoautotrophicum on H2 & CO2: High CH4 productivities in continuous culture.

498   Biomass 21, 315–321.

499   26. Petersson, A., Holm-nielsen, J.B., Baxter, D., 2007. Biogas upgrading technologies –

500   developments and innovations. IEA Bioenergy report.

501   27. Rittman, B., 2001. Environmental biotechnology: principles and applications. McGraw

502   Hill, New York.

503   28. Schönheit, P., Moll, J., Thauer, R.K., 1980. Growth Parameters (Ks, μ_{max}, Ys) of

504   Methanobacterium thermoautotrophicum. Arch. Microbiol. 65, 59–65.

505   29. Speece, R.E., 2008. Anaerobic biotechnology and odor/corrosion control for

506   municipalities and industries. Archaea Press.

507   30. Strevett, K.A., Vieth, R.F., Grasso, D., 1995. Chemo-autotrophic biogas purification for

508   methane enrichment: mechanism and kinetics. Chem. Eng. J. Biochem. Eng. J. 58, 71–79.

509   31. Ullman, F., 2000. Ullmann's Encyclopedia of Industrial Chemistry, 7th ed. Wiley,

510   Weinheim.

511   32. Wang, W., Xie, L., Luo, G., Zhou, Q., Angelidaki, I., 2013. Performance and microbial

512   community analysis of the anaerobic reactor with coke oven gas biomethanation and in situ

513   biogas upgrading. Bioresour. Technol. 146, 234–9.

514   33. Wilke, C.R., Chang, P., 1955. Correlation of diffusion coefficients in dilute solutions.

515   AIChE J. 1, 264–270.

516   34. Yang, H., Xu, Z., Fan, M., Gupta, R., Slimane, R.B., Bland, A.E., Wright, I., 2008.

517   Progress in carbon dioxide separation and capture: a review. J. Environ. Sci. (China) 20,

518   14–27.

519   35. Yu, Y., Ramsay, J.A., Ramsay, B.A., 2006. On-line estimation of dissolved methane

520   concentration during methanotrophic fermentations. Biotechnol. Bioeng. 95, 788–793.

Table 1

	I					II	III		IV	V	VI	
	a	b	c	d	e		a	b			a	b
t (d)	0	3	7	13	19	27	40	58	75	98	111	124
OLR ($m_{H_2}^3/m_R^3 d$)			10.1			20.1		30.2	45.2	25.1		40.2
$Q_{RC,G}$ (m³/d)	0.10	0.20	0.40	0.80	1.61	1.61	1.61	2.41	4.83	2.17	4.43	4.83

Table 1. Operating conditions applied during the study.

Figure1
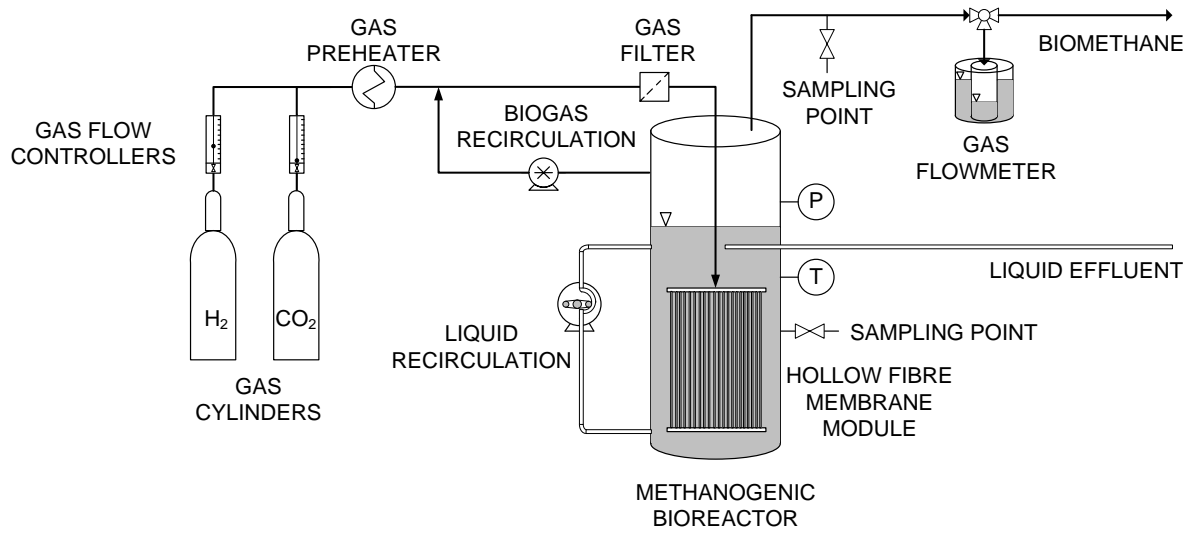
Figure 1. Pilot plant diagram

Figure2
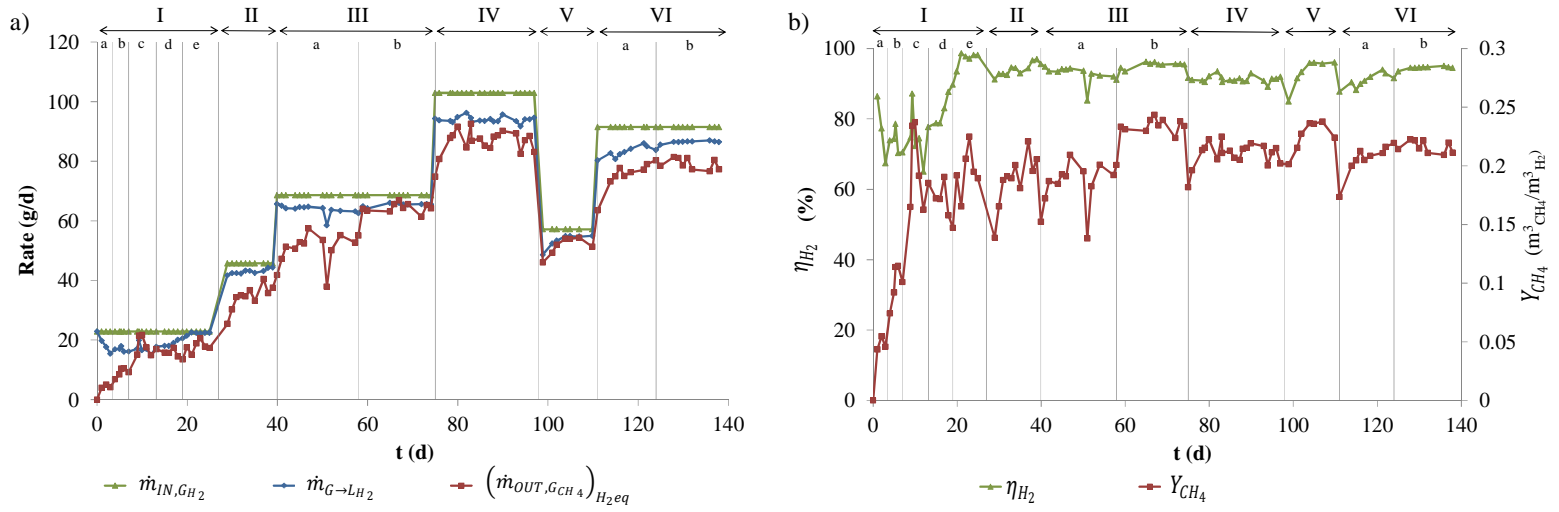
Figure 2. Performance of the bioconversion throughout the experiment. H_2 and CH_4 as equivalent H_2 mass flow rates (a). Efficiency of H_2 utilization and CH_4 yield (b).
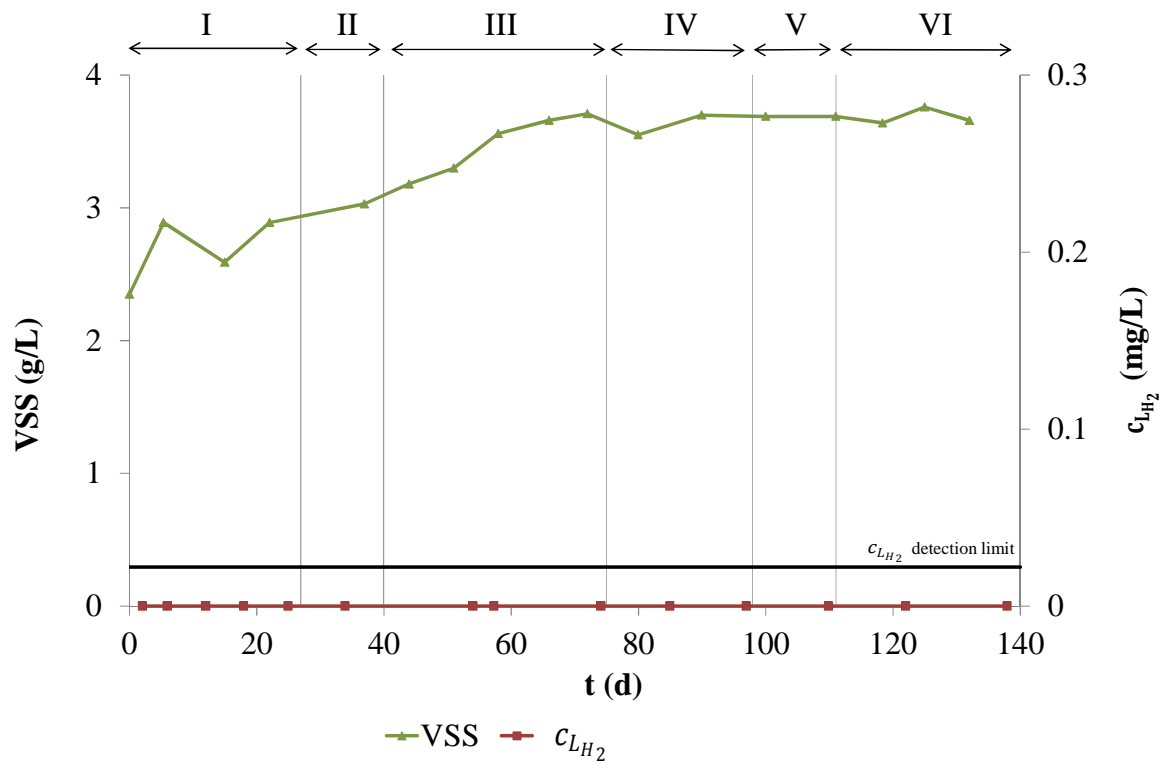
Figure3

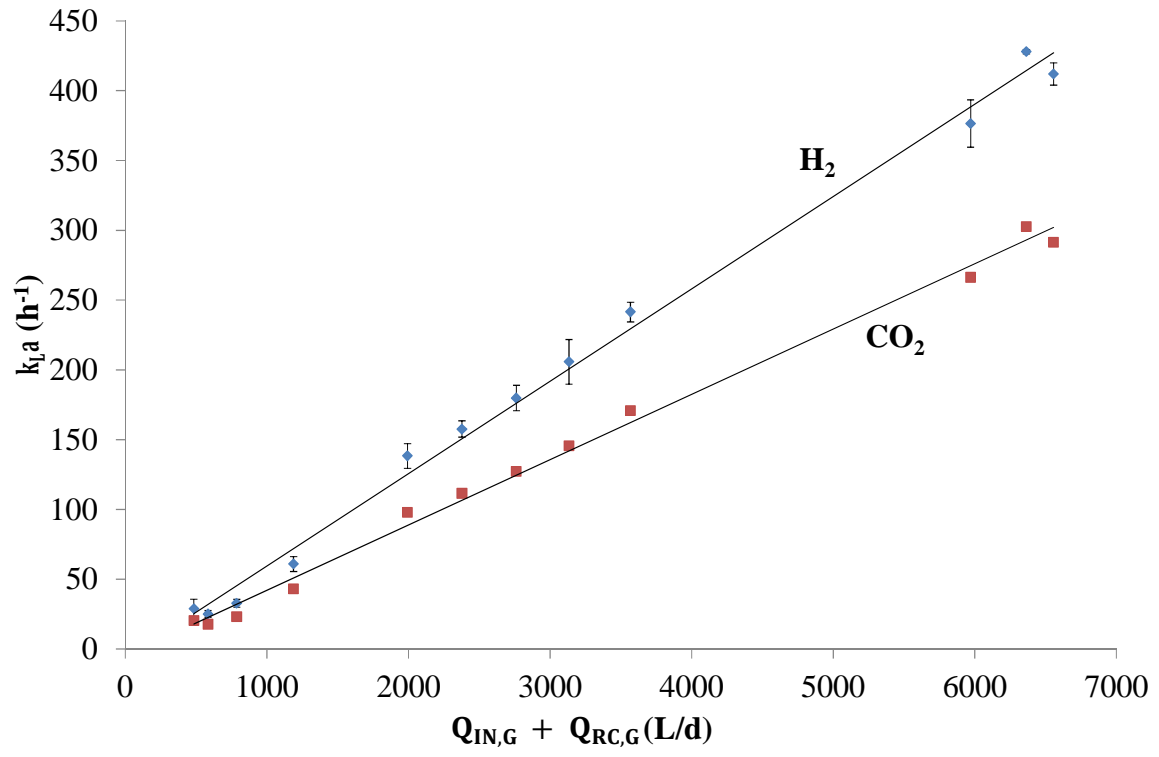Figure 3. VSS and dissolved H$_2$ concentrations in the bioreactor.

Figure4

Figure 4. Linear fitting of experimental $k_L a_{H_2}$ and estimated $k_L a_{CO_2}$ values.
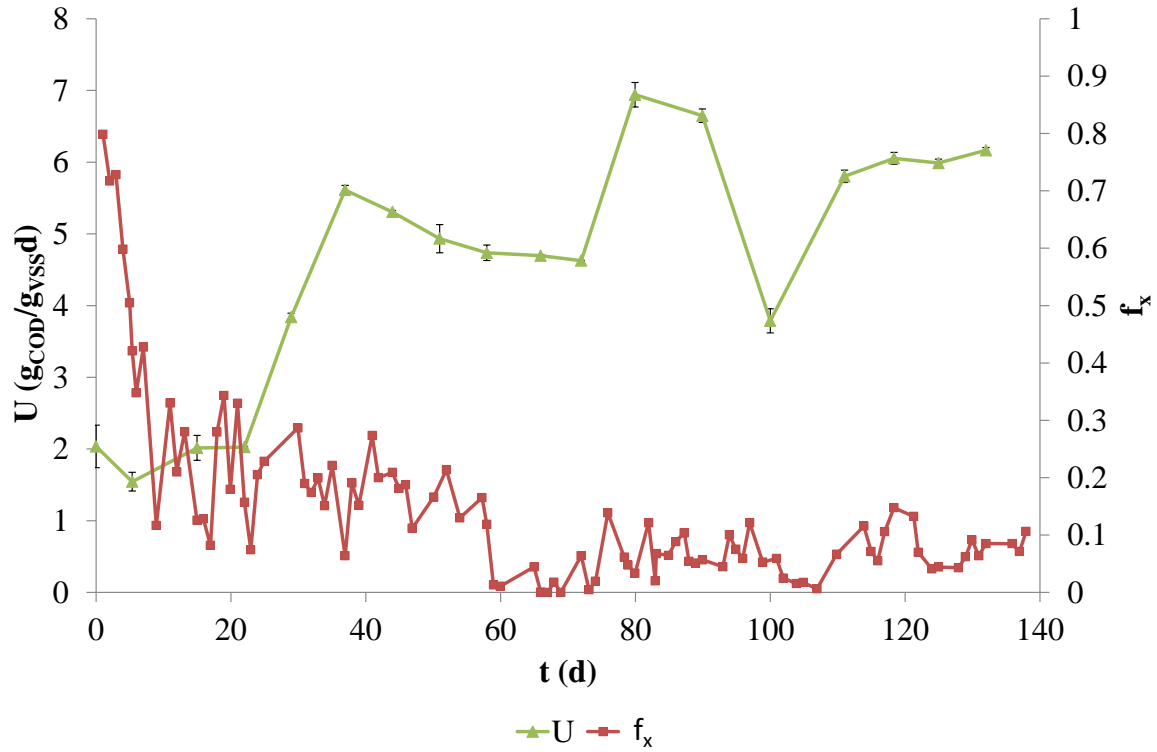
Figure5

Figure 5. Specific H_2 utilization rate (U) and fraction of H_2 employed for microbial growth during the experiment.
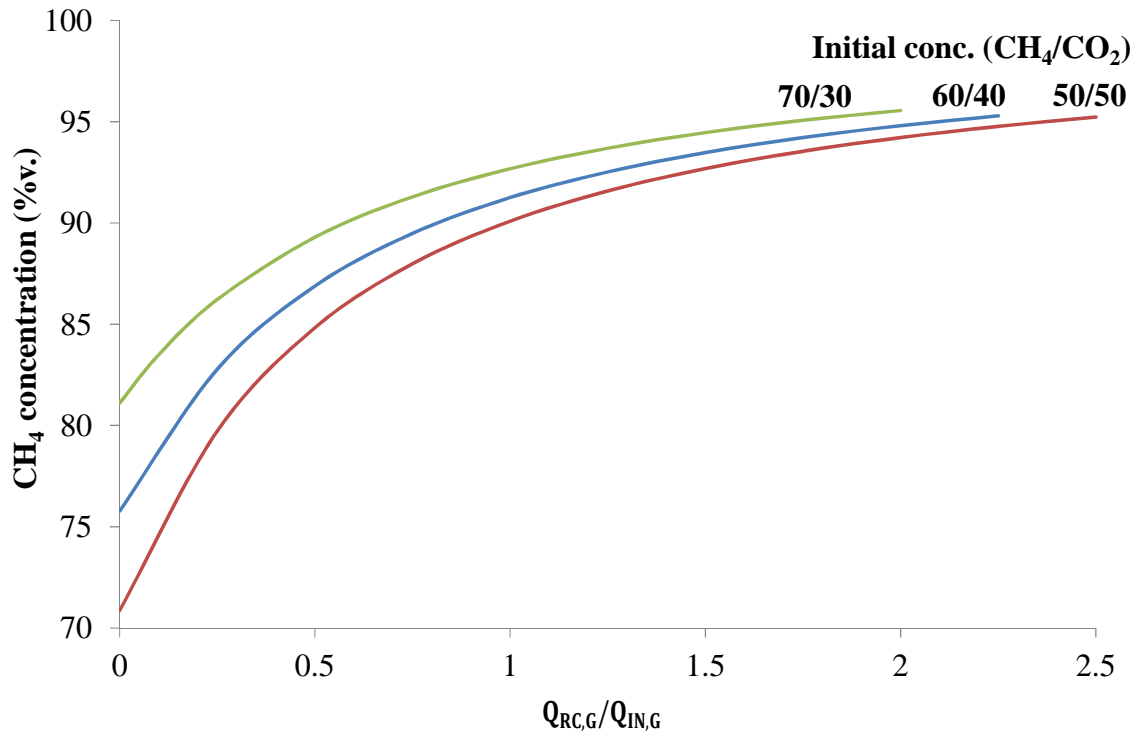
Figure6

Figure 6. Simulation of the final CH_4 concentration in upgraded biogas for equivalent CO_2 rates to those of the study.